Regular Article

PHYSICAL CHEMISTRY RESEARCH
Published by the
Iranian Chemical Society
www.physchemres.org
info@physchemres.org

***Phys. Chem. Res.**, Vol. 7, No. 4, 751-764, December 2019*
DOI: 10.22036/pcr.2019.183986.1628

Probing the Binding of Valacyclovir Hydrochloride to the Human Serum Albumin

D. Mohammad-Aghaie[a,*], M.N. Soltani Rad[a], R. Yousefi[b], N. Parvizi[a], S. Behrouz[a] and M.M. Alavianmehr[a]

[a]*Department of Chemistry, Shiraz University of Technology, Shiraz 71555-313, Iran*
[b]*Protein Chemistry Laboratory (PCL), Department of Biology, Shiraz University, Shiraz 71454, Iran*

(Received 8 May 2019, Accepted 10 September 2019)

UV-visible and Fluorescence spectroscopic methods were employed to study the interaction of human serum albumin (HSA) with Valacyclovir Hydrochloride. Additionally, molecular dynamics and molecular docking simulations were used to visualize and specify the binding sites of Valacyclovir Hydrochloride. The Stern-Volmer and van't Hoff equations along with spectroscopic observations were used to determine the binding and thermodynamic parameters. Overall, the obtained results revealed the presence of dynamic type of quenching mechanism in binding of Valacyclovir Hydrochloride to HSA, while the interaction was found to be entropy driven at domain III of HSA. Analyzing the protein ligand interactions with LIGPLOT confirmed the dominance of hydrophobic interactions, while the hydrogen bonding interactions play the minor role.

Keywords: Human serum albumin, Fluorescence spectroscopy, Molecular dynamics simulation, Valacyclovir hydrochloride

INTRODUCTION

Human Serum Albumin (HSA), the most abundant soluble protein in blood plasma, serves as a transport protein for a wide variety of endogenous and exogenous compounds. Among the four aspects of pharmacokinetics (adsorption, distribution, metabolism and excretion), HSA controls the distribution, because most drugs bind reversibly and with high affinity to albumin [1,2]. HSA contains a single 66 kDa polypeptide chain of 585 amino acids, which is stabilized by 17 disulphide bridges [3,4].

The globular structure of HSA is largely helical composed of three homologous domains (I, II and III). Each domain contains 10 helices divided into subdomains A and B, consisting of six and four α-helices, respectively [2,5].

The main ligand binding sites are known to be located in the hydrophobic pockets of subdomains, IIA and IIIA. These two subdomains are called warfarin and diazepam binding sites, which later denoted as site I (placed in IIA subdomain) and site II (placed in IIIA subdomain), according to Sudlow *et al.* [6-10]. Aromatic and heterocyclic ligands are found to bind within these two hydrophobic pockets. Seven binding sites are localized for fatty acids in sub-domains IB, IIIA, IIIB and on the subdomain interfaces. This protein also has a high affinity metal binding site at the N-terminus. Possessing multiple binding sites underlies the exceptional ability of HSA to interact with many organic and inorganic molecules, which in turn makes the HSA an important regulator of intercellular fluxes, as well as the pharmacokinetic behavior of many drugs [11,12].

The presence of single Trp residue in the primary structure of HSA is particularly advantageous in binding experiments, using fluorescent probes [3]. The Trp residue plays an important role as a chromophore and a fluorophore in optical studies of proteins [13].

Valacyclovir Hydrochloride (*i.e.*; L-valine-2-[(2-amino-1,6-dihydro-6-oxo-9-hipurin-9-yl)methoxy]ethyl ester Hydrochloride) (Fig. 1), is the prodrug (L-valinyl ester) of acyclovir and fully established antiviral drug

*Corresponding author. E-mail: d_aghaie@sutech.ac.ir

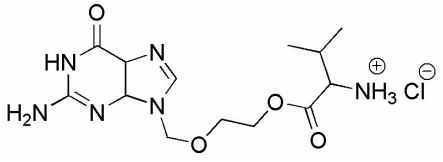

Fig. 1. The chemical structure of Valacyclovir.

exhibiting potent antiviral activity against herpes simplex virus types, 1 (HSV-1) and 2 (HSV-2) and vericellazoster virus (VZV) [14]. After oral administration, valacyclovir is rapidly hydrolyzed to acyclovir as a result of hepatic metabolism [15]. It provides a unique mechanism of enhancing the oral bioavailability of the parent compound, acyclovir. The main advantage of valacyclovir is higher concentration of acyclovir in the bloodstream, without added toxicity. Thus valacyclovir requires less frequent dosing than acyclovir.

Antiviral agents reduce viral replication by inhibiting viral DNA synthesis, required to reproduce itself. This helps to keep the virus inactive or "sleeping". Acyclovir is selectively phosphorylated only within virus-infected cells by viral thymidine kinase (TK). Further phosphorylation by cellular enzymes leads to the production of acyclovir triphosphate, which competes with the natural nucleotide, dGTP, resulting in the selective inhibition of viral DNA polymerase. Incorporation of the analogue triphosphate into the growing DNA chain, prevents continued extension of this chain [16-18].

For several years, the interaction of HSA with different drugs has been the subject of great amount of research projects. This is due to the important role of insulin-drug binding in pharmacology and pharmacodynamics [19].

Zhang *et al.* studied the molecular interactions and the intrinsic binding mechanisms of four benzophenone-type UV filters (BP-1, BP-2, BP-3 and BP-8) with HSA by combined spectroscopic and molecular docking techniques. Their study revealed that four studied benzophenones bind potently at site II of HSA and significantly quench its fluorescence, through the static quenching mechanism. Based on the thermodynamic parameters, the hydrogen bonding and van der Waals interactions were found to be the dominant interactions between BP-8 and HSA, while hydrophobic and electrostatic interactions had the main contribution to the interactions of BP-1, BP-2 and BP-3 with HSA [20].

Later, Zhuang *et al.* investigated the interactions of benzotriazole UV stabilizers (BZTs) with human serum albumin by a novel HSA biosensor, circular dichroism spectroscopy, fluorescence spectroscopy and MD simulation. They found that all BZTs bind tightly to HSA at Sudlow site I, while the perturbed microenvironment of this site and the impaired secondary structures of HSA by BZTs may cause potential structural damages of HSA, and hence may lead to the disturbance of its normal biological functions. Electrostatic interactions were revealed as the critical contributor to the various interactions between BZTs and HSA [21].

In our research group, Yousefi *et al.* [22] have studied the interaction of Dimethylplatinum(II) complex (Pt(II) complex) with DNA and HSA, using UV-Vis and fluorescence spectroscopies, along with molecular dynamics and molecular docking simulations. The molecular simulation and spectroscopic results were employed to characterize the interaction of aforementioned complex with HSA. Later in 2014, Alavianmehr *et al.* [23] applied the same method to probe the binding of thioTEPA to HSA, where they found that the enthalpy driven interaction occurs at domain 1 of HSA, through a mixed quenching mechanism.

In continuation of our previous works, here, the interaction of valacyclovir HCl with HSA was investigated through UV-Vis and Fluorescence spectroscopies. The Stern-Volmer and van't Hoff equations were used then to define the binding mechanism and parameters. Also, molecular dynamics and docking simulations (at 310 K) were performed to determine thermodynamic parameters and specify the binding sites. Furthermore, in order to understand the new structural features, induced by Valacyclovir, the (HSA-Valacyclovir HCl) complex was subjected to the molecular dynamics simulation and docking analysis.

EXPERIMENTAL

Materials

HSA was purchased from Sigma-Aldrich (St. Louis, MO, USA) and used without further purification. Potassium phosphate was used in analytical grade. The stock solutions

of HSA (10 μM) and Valacyclovir-HCl (0.5 mM) were prepared separately by dissolving the solid substances in 0.1 M potassium phosphate buffer (pH 7.4) [13]. All solutions were made in the double-distilled water.

Methods

UV-visible spectroscopy. Absorption of ultraviolet and visible radiation in organic molecules is restricted to certain functional groups (chromophores) containing valence electrons of low excitation energy.

Most absorption spectroscopy of organic compounds is based on transitions of n or π electrons to the π* excited state, due to the fact that the absorption peaks for these transitions fall in an experimentally convenient region of the spectrum (200-700 nm).

These transitions need an unsaturated group in the molecule to provide the π electrons. Here, the absorption measurements were performed on both pure HSA and HSA-Valacyclovir HCl complex, using $T90^+$ double beam scanning UV-Vis spectrophotometer instrument (PG Instrument Ltd., UK) equipped with Peltier Temperature Controller (Model PCT 2), in the range of 250-290 nm.

In the case of HSA-Valacyclovir HCl, the absorption titration experiments were carried out by maintaining HSA concentration fixed at 10 μM^{-1}, while varying the drug concentration by successive additions of 0.5 mM^{-1}, Valacyclovir HCl solution.

Fluorescence spectroscopy. HSA fluorescence intensity was measured by a Cary-Eclipse spectrophotometer (Varian, Australia) equipped with 1 cm path length quartz cell at various temperatures, using the source lamp voltage of 600 V.

The excitation and emission slit widths of 5nm were used for the fluorescence quenching experiment. The measurement of conventional spectra was performed by titrating 1.01 ml of 10 μM HSA, with microinjection of Valacyclovir HCl solution.

Fluorescence spectra were recorded at 302, 305 and 310 K upon excitation at 295 nm with 300-500 nm emission wavelengths for the conventional spectroscopies.

Molecular Dynamics Simulations

MD simulation of HSA protein. In order to obtain the HSA structure in a pseudo-physiological conditions, the crystal structure of this protein (PDB ID: 1AO6) [24] was downloaded from the protein data bank and subjected to the molecular dynamics simulation at appropriate temperature and pressure. This protein has two identical chains, therefore, it is adequate to perform the MD simulation on one chain only.

Taking advantage of pdb2gmx command in the GROMACS 4.5.4 simulation package [25], enabled us to generate appropriate topology file for HSA structure, based on the GROMOS 9643a1 force field [26]. This force field represents the non-bonded interactions as a sum of Lennard-Jones (LJ) and pairwise Columbic potentials, and computes the long-range electrostatic force, through the particle mesh Ewald Summation (PME) method [27].

In order to neutralize the negative charges on the protein molecule, 15 sodium ions were added to the system. After protein solvation in a cubic box, filled by SPC water molecules [28] and energy minimization with the steepest descent method for 100 ps, two equilibration phases in NVT and NPT ensembles, made the system ready for further submission to 15 ns MD simulation, at 310 K and 1 bar.

Berendsen thermostat and barostat were employed to keep the temperature and pressure constant, while the cut-off values for van der Waals and Coulombic interactions were fixed at 1.4 Å.

The output structure of the MD simulation was later docked into the Valacyclovir HCl (More on this in molecular docking section).

MD simulation of HSA valacyclovir HCl complex. MD simulation study of HSA, in complex with Valacyclovir HCl, was performed at the same conditions, as for HSA itself. The required topology and coordinates for Valacylovir HCl were obtained from GlycoBioChem PRODRG2 Server [29], while HSA topology and interaction parameters were created using the standard GROMOS96 43a1 force field [26].

The energy minimization, equilibration, and MD steps were performed at similar conditions, employed for the pure HSA simulation.

Molecular Docking

The HyperChem Professional 7.0 software was used for the structural optimization of Valacyclovir HCl [30]. Energy minimization of the drug was performed by AM1,

semi empirical method, with Polak-Ribiere algorithm, until the root mean square gradient reached 0.01 kcal mol^{-1}.

Afterward, we used the Gussaian 09 software at the B3LYP/6-31g computational level, to ensure that the drug has achieved its global minimum [31].

The energy minimized structure of Valacyclovir HCl was docked into the equilibrated HSA structure (obtained from MD simulation at 310 K), employing the Auto Dock Vina docking server [32].

RESULTS AND DISCUSSION

Spectral Measurements

UV-Vis absorption studies. UV-Vis absorption spectroscopy is a simple and promising method to investigate structural changes in protein and explore the complex formation.

In proteins, the peptide bonds absorb light in the "far-UV" range of 180-230 nm. The resulting peak is an indication of the π-π* transition of characteristic polypeptide backbone structure of C=O.

On the other hand, the aromatic residues, tyrosine (Tyr), tryptophan (Trp), and phenylalanine (Phe), also absorb light in this region and, in addition, show bands near 260 to 280 nm (in the near-UV range), where corresponding peaks are attributed to the n-π* transitions of aromatic amino acids [33].

Based on the pdb entry code 1AO6, our selected HSA structure contains one Trp (Trp 214), 18 Tyr and 32 Phe residues.

In this paper, we have employed the UV-Vis absorption spectroscopy at around 280 nm, to specify the probability and quality of complex formation between HSA and Valacyclovir HCl, where the resulting spectra are depicted in Fig. 2.

For this purpose, HSA concentration was kept fixed at 10 μM, while those of Valacyclovir-HCl were 0, 4.95, 9.804, 14.653, 19.23, 23.801, 28.302, 32.710 and 37.037 μM, for the systems indicated by curves "a" to "i", respectively.

Inspecting Fig. 2 reveals that HSA gives a strong absorbance peak at 280 nm, while further stepwise additions of Valacyclovir-HCl result in gradual reductions in peak intensity, along with the movement of peak position to the higher wavelengths (red shift).

Obvious changes in the absorbance peak intensity and position illustrate that the interaction between HSA and Valacyclovir-HCl induces some disturbances to the microenvironment around the aromatic aminoacids [34]. Due to the complex formation between HSA and Valacyclovir-HCl, the band gap between ground state and excited state in the n-π* transition (in aromatic aminoacids) has been decreased, so the corresponding absorbance peak has moved slightly towards higher wavelengths (red shift).

Fluorescence Quenching

Quenching of fluorescence is a physicochemical process that decreases fluorescent intensity of light emitting molecules. There is a wide variety of quenching processes including excited-state reactions, molecular rearrangements, ground-state complex formation, and energy transfer.

In HSA, the fluorescence emission spectra is mainly due to the presence of Trp 214 in the subdomain IIA. In this study, the conventional fluorescence spectroscopy was employed to explore the HSA-Valacyclovir HCl interaction.

Conventional fluorescence spectroscopy. Excitation of Trp 214 in subdmain IIA of HSA, at 295 nm, through conventional fluorescence quenching, provides information on the conformational changes of the protein [35].

Figure 3 shows that the fluorescence intensity of HSA is reduced through successive additions of Valacyclovir HCl, while no shift in the position of maximum emission wavelength is observed. This observation indicates that Valacyclovir-HCl does not alter the polarity around the fluorophore.

It is known that the fluorescence intensity of HSA is affected by its environment, in a way that even a small change in the local surrounding of HSA changes its fluorescence intensity [36]. Although Fig. 3 confirms the quenching of fluorescence spectra of HSA in presence of studied drug, lack of red or blue shift in peak position is an indication of no conformational alteration in HSA molecule. It is worth mentioning that higher concentrations of Valacyclovir-HCl may ultimately give rise to the recordable changes.

Quenching mechanism. The quenching phenomenon can result from collisional encounters between the

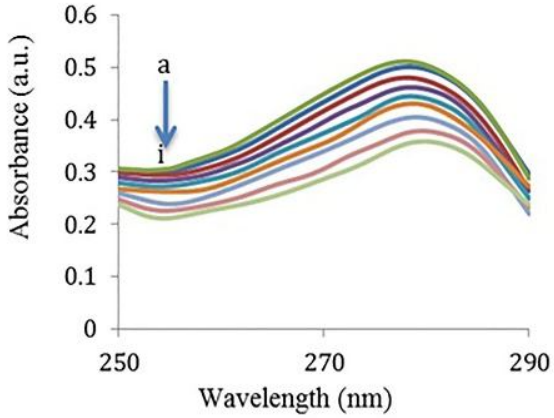

Fig. 2. UV-visible absorbance spectra of Valacyclovir HCl binding to HSA at 298 K and different concentrations of Valacyclovir HCl (a-i): 0, 4.95, 9.804, 14.653, 19.23, 23.801, 28.302, 32.710 and 37.037 µM.

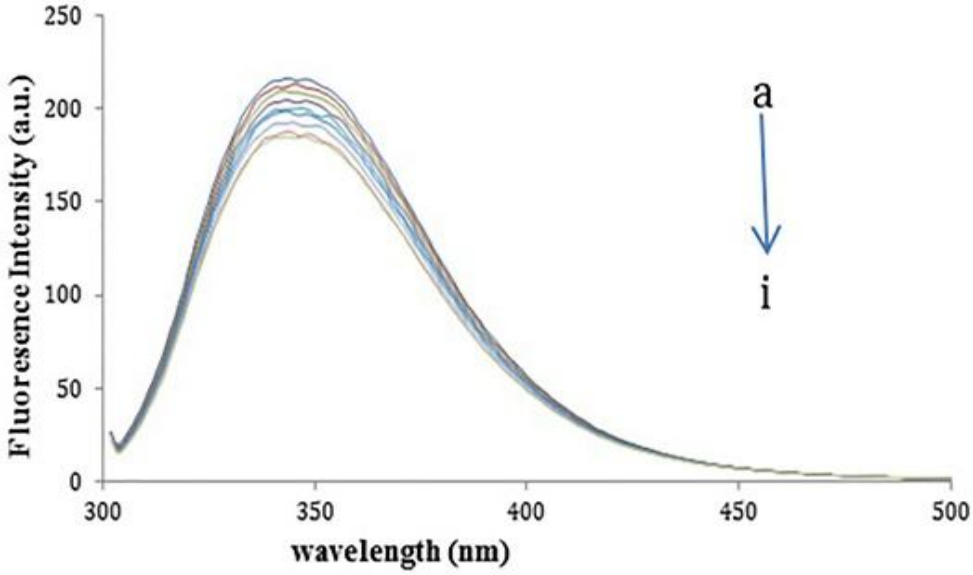

Fig. 3. Conventional fluorescence spectra of HSA at 302 K, (HSA: 10 µM and Valacyclovir HCl (a-i): 0, 4.95, 9.804, 14.653, 19.23, 23.801, 28.302, 32.710 and 37.037 µM).

fluorophore and quencher**,** called collisional or dynamic quenching. The other possible mechanism is static quenching providing valuable information about binding between the fluorescent sample and the quencher. Both static and dynamic quenching require molecular contact between the fluorophore and quencher.

In the case of collisional quenching, the quencher must diffuse to the fluorophore during the lifetime of the excited state. Upon contact, the fluorophore returns to the ground state without emission of a photon. In general, quenching occurs without any permanent change in the molecules; that is, without a photochemical reaction. In static quenching, a

complex is formed between the fluorophore and the quencher, and this complex is nonfluorescent [36].

These two quenching mechanisms are distinguishable based on their different temperature dependent behaviour. In the case of dynamic quenching, an increase in temperature leads to an increase in the diffusion constant of the quencher leading to an increase in collisional quenching. In contrast, the temperature elevation destabilizes the fluorophore-quencher complex and so decreases the value of static quenching constant [36].

It is common to use the Stern-Volmer relationship and the corresponding plots in order to specify the quenching mechanism [37]:

$$\frac{F_0}{F} = 1 + k_q \tau_0 [Q] = 1 + K_{SV}[Q] \quad (1)$$

Here, F_0 and F, respectively represent the fluorescence intensities in the absence and presence of quencher, with the [Q] concentration.

K_{SV} is the Stern-Volmer quenching constant, k_q the biomolecular quenching rate constant, and τ_0 the average life-time of the biomolecule in the quencher absence, with a value of 10^{-8} s for HSA [38].

Since both static and dynamic quenching result in a linear Stern-Volmer plots, they cannot be distinguished by a single experiment; however, they are distinguished by their different dependences on temperature, viscosity, and/or lifetime measurements.

In order to obtain the Stern-Volmer quenching constants (K_{SV}) at different temperatures, the F_0/F values were plotted against [Q] and the corresponding slopes were calculated (Fig. 4).

These plots should yield an intercept of unity on the y-axis and a slope equal to K_{SV}. It is useful to note that $1/K_{SV}$ is the quencher concentration at which $F_0/F = 2$ or 50% of the intensity is quenched. Inspection of K_{SV} values (reported in Table 1) as a function of temperature, suggests the presence of dynamic quenching mechanism.

Binding and thermodynamic parameters. The parameters characterizing the binding process, the enthalpy change (ΔH), entropy change (ΔS) and Gibbs free energy change (ΔG), constitute the main evidences for determining the forces acting between Valacyclovir HCl and HSA.

These forces can be hydrophobic, Van der waals, hydrogen bonding and/or electrostatic interactions [39]. When small molecules bind independently to a set of equivalent sites on a macromolecule like protein, the equilibrium between free and bound molecules is given by the following equation [40,41]:

$$\log \frac{(F_0 - F)}{F} = \log K_b + n \log[Q] \quad (2)$$

where F_0 and F are the fluorescence intensities in the absence and presence of Valacyclovir-HCl, respectively. K_A is the binding constant for a set of sites, and n is the average number of binding sites per HSA.

In this study, the fluorescence quenching data for the interaction of Valacyclovir-HCl and HSA were analyzed and $\log(F_0 - F/F)$ was plotted *versus* log[Q].

Consequently, a straight line was obtained, whose slope is equal to n and the intercept on the y-axis yields $\log K_A$. Close inspection of the results (reported in Table 1) shows that *n* increases with increasing temperature. This behavior can be attributed to the more accessibility of HSA binding sites due to the higher diffusion rate, where HSA conformation changes in a way to have more interactions with the drug. On the other hand, considering the n values indicate each Valacyclovir-HCl molecule, binds to one molecule of HSA at the studied temperatures. The binding affinity values of HSA for Valacyclovir-HCl are extremely low (approximately on the order of 10^3 M^{-1}, all data are included in Table 1).

It is worth mentioning that the high affinity binding constants of ligand-protein interactions lie in the range of 10^6-10^8 M^{-1} [42]. Therefore, the interaction of HSA and Valacyclovir-HCl is considered as a poor one.

Dependence of the binding constants on the temperature confirms that a thermodynamic process is responsible for the complex formation [43].

In this respect, the temperature dependence of the thermodynamic parameters was examined to characterize the driving forces between Valacyclovir-HCl and HSA.

The thermodynamic binding parameters can be easily determined by van't Hoff equation:

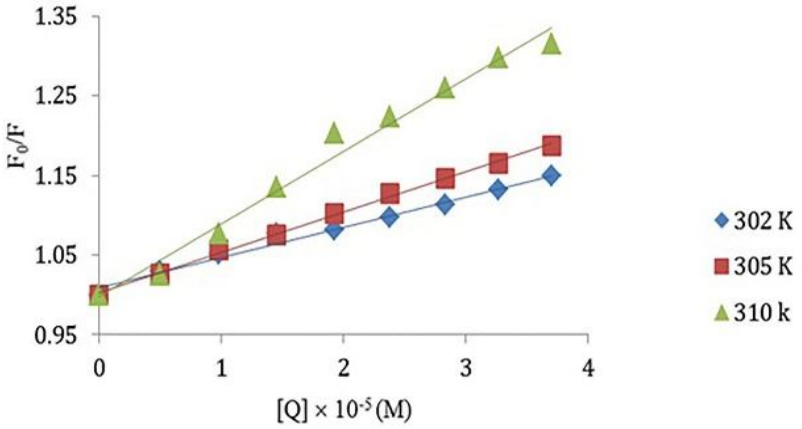

Fig. 4. Stern-Volmer curves of fluorescence quenching of HSA at different temperatures.

Table 1. Quenching, Binding and Thermodynamic Parameters of HSA-Valacyclovir-HCl Interactions

T (K)	K_{SV} ($\times 10^3$ M^{-1})	n	logK ($\times 10^3$ M^{-1})	ΔG (kJ mol^{-1})	ΔH (kJ mol^{-1})	ΔS (J mol^{-1} K^{-1})	R^2
302	3.7803 ± 0.14	0.7824 ± 0.03	2.626 ± 0.004	-15.166	551.931 ± 7.073	1.812 ± 0.0009	0.9909
305	5.0390 ± 0.13	0.9648 ± 0.01	3.5538 ± 0.006	-20.743			0.9979
310	9.1210 ± 0. 9	1.2445 ± 0.08	5.0878 ± 0.01	-30.156			0.9738

$$\ln K = -\frac{\Delta H}{RT} + \frac{\Delta S}{R} \quad (3)$$

or using the equations:

$$\Delta G = -RTknK \quad (5)$$

where R is the global gas constant, equal to 8.3144621 J mol^{-1} K^{-1}. All calculated thermodynamic parameters are summarized in Table 1.

The same as any other spontaneous process, binding occurs only when it is associated with a negative Gibbs free energy (ΔG < 0) [44]. It is possible to specify the binding mechanism between HSA protein and drug, based on the ΔH and ΔS signs of the system [45].

When both ΔS and ΔH values are negative, van der Waals and hydrogen bonding interactions are the dominant forces. On the other hand, ΔS > 0 along with ΔH < 0 confirm the presence of electrostatic interactions, while when both ΔS and ΔH values are positive, the main forces acting between protein and drug are the hydrophobic ones [44].

In this study, the negative ΔG values demonstrate the spontaneity of the interaction, while the positive enthalpy and entropy values indicate that the HSA-Valacyclovir HCl interaction is entropy driven, meaning that the binding signature is dominated by the classical hydrophobic effects. On the other hand, the positive ΔH value shows that the reaction is endothermic [46].

Molecular Dynamics Simulation

Two independent molecular dynamics simulations were performed on HSA and also HSA-Valacyclovir HCl complex, in order to obtain and analyze their structures,

under pseudo-physiological conditions.

It is worth mentioning that the quenching phenomenon always requires a molecular contact between the fluorophore and the quencher. Collisional (dynamic) quenching occurs when the excited fluorophore experiences contact with an atom or molecule that can facilitate non-radiative transitions to the ground state. On the other hand, in some cases, the fluorophore can form a stable complex with another molecule. If this ground-state is non-fluorescent, then we say that the fluorophore has been statically quenched. As mentioned before, in the case of Valacyclovir Hydrochloride, the HSA fluorescence quenches through the dynamics quenching mechanism and no stable complex is formed between the human serum albumin and the studied drug.

Considering that the dynamic quenching requires a collision between the fluophore and the quencher, we can assume that a momentary (short-lived) complex is formed between the HSA and Valacyclovir-Hydrochloride. This is the reason behind simulating the HSA-Valacyclovir HCl complex, in this study.

Analyzing the time dependence changes of backbone RMSD serves as a promising tool to determine the stability and the state of the simulated system. In bioinformatics, the root mean square deviation (RMSD) of atomic positions is a measure of the average distance between the atoms (usually the backbone atoms) of the superimposed proteins. This property is calculated through the following equation, where $r_i(t)$ and r_i^{ref} are the positions of atom i at time (t) of the simulation, and in a reference structure, respectively.

$$RMSD(t) = \left[\frac{1}{M} \sum_{i=1}^{N} (m_i(r_i(t)) - r_i^{ref})^2 \right] \quad (6)$$

Where M = $\sum$ m_i and $r_i(t)$ is the position of atom i at time t after least square fitting of the structure to the reference [47].

Figure 5 illustrates that the backbone RMSD of free HSA at 310 K rises first and then fluctuates around the average value of 0.36 nm, mainly after 8000 ps of the simulation time, where it remains almost constant afterwards. This can be interpreted as an evidence for obtaining a quasi-equilibrium state for HSA.

Analyzing the molecular dynamics simulation results of combined protein-drug system reveals that the backbone RMSD of HSA-Valacyclovir HCl complex oscillates around 0.47 nm (again after 8000 ps), where the oscillations are higher in comparison to the pure HSA system.

In other words, comparing the RMSD plots for HSA, both in pure form and in complex with the drug, shows that the root mean square deviation of HSA backbone increases in the complex form, which can be an indication of unstable complex between these two entities.

We also analyzed the radius of gyration for both HSA and HSA-Valacyclovir HCl complex. Gyration radius (R_g) of protein is a measure of its compactness. Figure 6 demonstrates the R_g values during 15000 ps simulation time for both of the studied systems. In both cases, the R_g values were almost stabilized at about 9000 ps, indicating that the MD simulations have achieved quasi equilibrium state after this time.

The initial value of Rg was about 2.56 nm for both systems. Close examination of Fig. 6 shows that the final R_g values become respectively 2.57 and 2.55 nm for HSA and HSA-Valacyclovir HCl complex. Although the difference is negligible, it seems that HSA tends to adopt more compact structure when facing to the Valacyclovir Hydrochloride.

Secondary Structural Changes

In addition to the common method of circular dichroism, to study the secondary structure of proteins, there are also in silico tools which are able to elucidate further details. The DSSP program works by calculating the most likely secondary structure assignment, given the 3D structure of a protein. It does this by reading the position of the atoms in a protein (the ATOM records in a PDB file) followed by calculation of the H-bond energy between all atoms. In addition to the secondary structure, dssp defines the geometrical features and solvent exposure of the proteins.

Assessment of dssp results for HSA structure with its 582 residues provides its intrinsic structural characteristics. On the other hand, secondary structure analysis of HSA complexed to Valacyclovir HCl reflects the induced structural changes in HSA protein, due to its interaction with the drug. Table 2 contains the information regarding the accessible surface area, hydrogen bonding and other structural features of HSA, in both pure and complex states.

Survey of dssp results indicates that the solvent

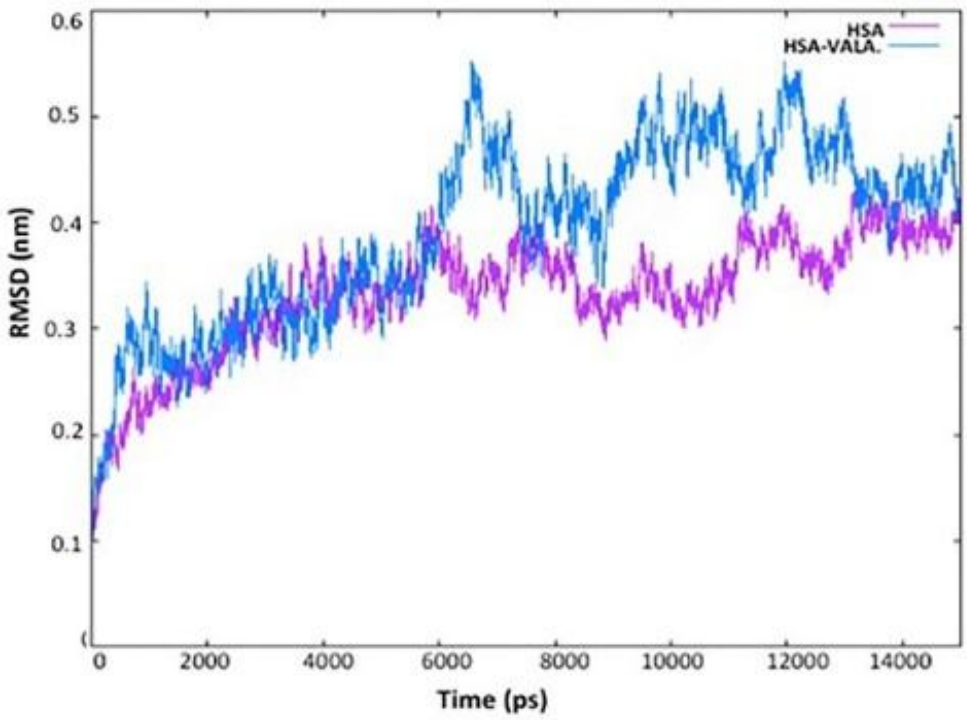

Fig. 5. Root mean square deviation (RMSD) of HSA backbone in the presence and absence of Valacyclovir HCl at 310 K.

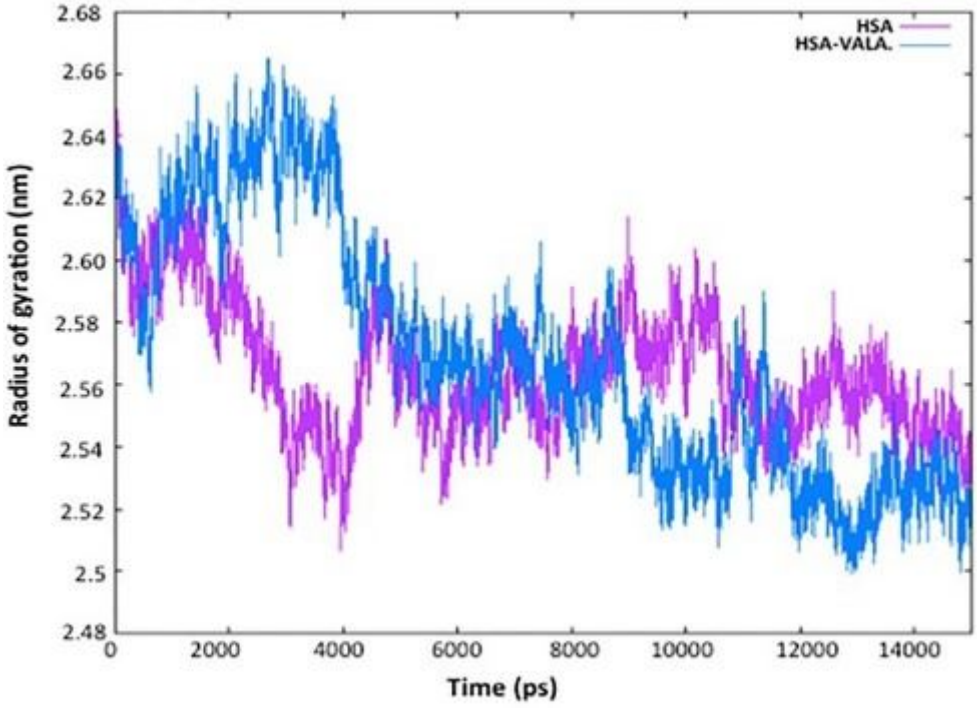

Fig. 6. Radius of gyration (Rg) of HSA backbone in the presence and absence of Valacyclovir HCl at 310 K.

Table 2. Structural Features of HSA in Pure and Complex States

Parameter	HSA	HSA in complex with Valacylovir-HCl
Accessible surface (Å^2)	26068.0	25645.0
Total number of H-bonds (O(I) → H-N)	436	441
Alphahelix	400	434
Residue in isolated beta-bridge	0	0
Extended strand, participates in beta ladder	0	0
3-helix (3/10 helix)	3	0
5-helix (pi helix)	0	0
Hydrogen bonded turn	42	33
Bend	50	38
Blank	111	72

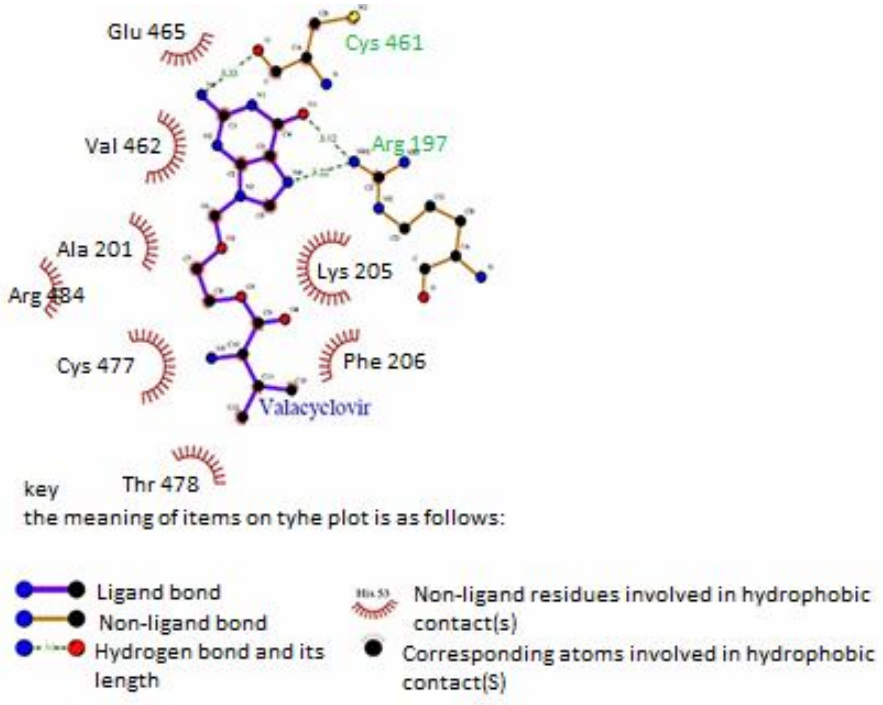

Fig. 7. Schematic representation of HSA and Valacyclovir HCl interactions taken from LIGPLOT program**.**

accessible area of HSA decreases in the complex state. This is compatible with the slightly lower Rg value of this protein in the vicinity of Valacyclovir HCl. The total number of H-bond alpha helices show an increase, while the "hydrogen bonded turns", 3 helices, and bends show a decrease in the complex state. In both states, there are

neither “extended residues shaped as beta ladder”, nor the amino acids in isolated beta bridge.

Molecular Docking Simulation

In order to specify the binding sites and conformation energies of HSA-Valacyclovir HCl complex, the AutoDock Vina software was employed. It has been reported that AutoDock-vina preforms faster than AutoDock 4, and is also able to acquire more accurate docking calculations [48].

AutoDock-vina needs both the receptor and ligand files in PDBQT format. First, the MGL Tools-1.5.6 was employed to remove all the water molecules surrounding the receptor [49]. Nonpolar hydrogen atoms were merged prior to adding the Kollman charges to the HSA crystal coordinate file. The center of the docking grid was set to x = 34.031, y = 60.792 and z = 58.913, with maximum spacing of 1 Å, where the grid-size was kept at 80 × 86 × 96 Å, to cover the entire receptor molecule. The 3D coordinate file of receptor was saved into PDBQT format. All other docking parameters were kept as the default.

AutoDock vina yielded 9 best conformations that are arranged in the order of increasing binding energies. The conformation with the lowest binding energy was chosen for further evaluation.

Binding site analysis was performed on the HSA-Valacyclovir HCl complex with the best binding affinity at 310 K after MD simulation. Valacyclovir HCl lies at domain IIIA of HSA. Ala 291, Trp 214, Arg 222, Glu 292, Lys 195, Lys 199, Asp 451 and Val 455 (Fig. 7) stabilize Valacyclovir HCl in its binding site through hydrogen bonding, hydrophobic contacts, and also steric interaction.

Later, the LIGPLOT [50], a program for automatically plotting protein ligand interactions, was employed to analyze the interactions between HSA and Valacyclovir HCl. This program was used to specify the interactions mediated by hydrogen bonds and hydrophobic contacts. (Fig. 7). Hydrogen bonds are indicated by dashed lines between the atoms involved, while hydrophobic contacts are represented by an arc with spokes radiating towards the ligand atoms they contact. The contacted atoms are shown with spokes radiating back.

CONCLUSIONS

In this study, the UV-Vis and conventional fluorescence spectroscopies, in combination with molecular dynamics and docking simulations were employed to study the molecular interactions of Valacyclovir Hydrochloride with HSA.

The Stern-Volmer and Van't Hoff equations were used to calculate the thermodynamic parameters and to specify the nature of binding. Our study revealed that the interaction of Valacyclovir-HCl with HSA is entropy driven occurring through a dynamic quenching mechanism at domain IIIA of HSA.

The thermodynamic parameters, $\Delta G^\circ < 0$, $\Delta H^\circ > 0$ and $\Delta S^\circ > 0$ at different temperatures indicated the spontaneity of the binding process, while the hydrophobic interactions played a major role in the interaction between Valacyclovir Hydrochloride and HSA.

This prediction was confirmed when we used LIGPLOT to analyze the protein ligand interactions. Therefore, we could schematically observe the dominance of hydrophobic interactions, while the hydrogen bonding interactions play the minor role.

Briefly, the combination of UV and fluorescence spectroscopic techniques, along with molecular dynamics and docking simulations, was adequate to decide on the nature of interactions between HSA and Valacyclovir-HCl.

Simultaneous assessment of the spectroscopic and simulation results demonstrated no significant change in the HSA structure, upon binding of low concentration of Valacyclovir-HCl. In other words, the presence of Valacyclovir-HCl does not promote any considerable change in the secondary structure of HSA, its polarity and hydrophobicity.

Consequently, its lifetime would decrease and its higher dosage must be supplied to the patient. This drug is mainly in its unbound form in the bloodstream and the lack of significant binding affinity to HSA can explain the requirement of its high dosage in treatment of infections caused by herpes viruses in adults.

REFERENCES

[1] Chemma, M. A.; Taboada, P.; Barbosa, S.; Juarez, J.;

Gutierrez-Pitchel, M.; Siddiq, M.; Mosquera, V., Human serum albumin unfolding pathway upon drug binding: A thermodynamic and spectroscopic description. *J. Chem. Thermodyn.* **2009**, *41*, 439-447, DOI: 10.1016/j.jct.2008.11.011.

[2] Yang, F.; Bian, C.; Zhu, L.; Zhao, G.; Huang, Z.; Huang, M., Effect of human serum albumin on drug metabolism: structural evidence of esterase activity of human serum albumin. *J. Struct. Biol.* **2007**, *157*, 348-355, DOI: 10.1016/j.jsb.2006.08.015.

[3] Artali, R.; Bombieri, G.; Calabi, L.; Del Pra, A., A molecular dynamics study of human serum albumin binding sites. *Farmaco* **2005**, *60*, 485-495, DOI: 10.1061/j.farmac.2005.04.010.

[4] Saber, M.A.; Stöckbauer, P.; Morávek, L.; Meloun, B., Disulfide bonds in human serum albumin. *Collect. Czech. Chem. Commun.* **1977**, *42*, 564-579, DOI: 10.1135/cccc19770564 .

[5] Fasano, M.; Curry, S.; Terreno, E.; Galliano, M.; Fanali, G.; Narciso, P.; Notari, S.; Ascenzi, P., The extraordinary ligand binding properties of human serum albumin. *IUBMB life* **2005**, *57*, 787-796, DOI: 10.1080/15216540500404093.

[6] Carter, D. C.; Ho, J. X., Structure of serum albumin. *Adv. Protein Chem.* **1994**, *45*, 153- 203, DOI: 10.1016/s0065-3233(08)60640-3.

[7] Bos, O. J. M.; Vansterkenburg, E. L. M.; Boon, J.C.I.; Fischer, M. J. E.; Wilting, J.; Janssen L. H. M., Location and characterization of the suramin binding sites of human serum albumin. *Biochem. Pharmacol.* **1990**, *40*, 1595-1599. DOI: 10.1016/006-2952(90)90460-3.

[8] Wilting, J.; Hart, B. J. T.; De Gier, J. J., The role of albumin conformation in the binding of diazepam to human serum albumin. *Biochem. Biophys. Acta* **1980**, *626*, 291-298, DOI: 10.1016/0005-2795(80)90123-3.

[9] Sudlow, G.; Birkett, D. J.; Wade, D. N., The characterization of two specific drug binding sites on human serum albumin. *Mol. Pharmacol.* 1975, *11*, 824-832.

[10] Sudlow, G.; Birkett, D. J.; Wade, D. N., Further characterization of specific drug binding sites on human serum albumin. *Mol. Pharmacol.* **1976**, *12*, 1052-1061.

[11] Petitpas, I.; Grune, T.; Battacharya, A. A.; Curry, S., Crystal structures of human serum albumin complexed with monounsaturated and polyunsaturated fatty acids. *J. Mol. Biol.* **2001**, *314*, 955-960, DOI: 10.1006/jmbi.2000.5208.

[12] Grelamo, E. L.; Silva, C. H. T. P.; Imasato, H.; Tabak, M., Interaction of bovine (BSA) and human (HSA) serum albumins with ionic surfactants: spectroscopy and modelling. *Biochem. Biophys. Acta* **2002**, *1594*, 84-99. DOI: 10.1016/S0167-4838(01)00287-4.

[13] Moriyama, Y.; Ohta, D.; Hachiya, K.; Mitsui, Y.; Takeda, K., Fluorescence behavior of tryptophan residues of bovine and human serum albumins in ionic surfactant solutions: A comparative study of the two and one tryptophan(s) of bovine and human albumins. *J. Protein Chem.* **1996**, *15*, 265-272, DOI: 10.1007/BF01887115.

[14] Ormrod, D.; Scott, L. J.; Perry, C. M., Valaciclovir: a review of its long term utility in the management of genital herpes simplex virus and cytomegalovirus infections. *Drugs* **2000**, *59*, 839-863, DOI: 10.2165/00003495-200059040-00013.

[15] Beutner, K. R., Valacyclovir: a review of its antiviral activity, pharmacokinetic properties, and clinical efficacy. *Antivir. Res.* **1995**, *28*, 281-290.

[16] O'Brien, J. J.; Campoli-Richards, D. M., *Acyclovir. Drugs* **1989**, *37*, 233-309, DOI: 10.2165/00003495-198937030-00002.

[17] Landowski, C. P.; Sun, D.; Foster, D. R.; Menon, S. S.; Barnett, J. L.; Welage, L. S.; Ramachandran, C.; Amidon, G. L., Gene expression in the human intestine and correlation with oral valacyclovir pharmacokinetic parameters. *J. Pharmacol. Exp. Ther.* **2003**, *306*, 778-786, DOI: 10.2165/jpet.103.051011.

[18] Elion, G. B., Acyclovir: Discovery, mechanism of action, and selectivity, *J. Med. Virol.* **1993**, *1*, 2-6, DOI: 10.1002/jmv.1890410503.

[19] Li, Y.; He, W. Y.; Liu, H. X.; Yao, X. J.; Hu, Z. D., Daidzein interaction with human serum albumin studied using optical spectroscopy and molecular modeling methods. *J. Mol. Struct.* **2007**, *831*, 144-150, DOI: 10.1016/J.MOLSTRUC.2006.07.034.

[20] Zhang, F.; Zhang, J.; Tong, C.; Chen, Y.; Zhuang, S.;

Liu, W., Molecular interactions of benzophenone UV filters with human serum albumin revealed by spectroscopic techniques and molecular modeling. *J. Hazard. Mater.* **2013**, *263*, 618-626, DOI: 10.1016/j.jhazmat.2013.10.024

[21] Zhuang, S.; Wang, H.; Ding, K.; Wang, J.; Pan, L.; Lu, Y.; Liu, Q.; Zhang. C., Interactions of benzotriazole UV stabilizers with human serum albumin: Atomic insights revealed by biosensors, spectroscopies and molecular dynamics simulations. *Chemosphere,* **2016**, *144*, 1050-1059, DOI: 10.1016/j.chemosphere.2015.09.085.

[22] Yousefi, R.; Alavianmehr, M. M.; Mokhtari, F.; Keshavarz, F.; Nabavizadeh, M.; Rashidi, Moosavi-Movahedi, A. A., Spectroscopic and molecular dynamics studies on binding of dimethylplatinum(II) complex drug to human serum albumin. *Bull. Chem. Soc. Jpn*. **2014**, *87*, 1094-1100.

[23] Alavianmehr, M. M.; Yousefi, R.; Keshavarz, F.; Mohammad-Aghaie, D., Probing the binding of thioTEPA to human serum albumin using spectroscopic and molecular simulation approaches. *Can. J. Chem.* **2014**, *92*, 1066-1073, DOI: 10.1139/cjc-2013-0571.

[24] Sugio, S.; Kashima, A.; Mochizuki, S.; Noda, M.; Kobayashi, K., Crystal structure of human serum albumin at 2.5 Å resolution. *Protein Eng.* **1999**, *12*, 439-446, DOI: 10.1093/protein/12.6.439.

[25] Pronk, S.; Páll, S.; Schulz, R.; Larsson, P.; Bjelkmar, P.; Apostolov, R.; Shirts, M. R.; Smith Peter, J. C.; Kasson, M., van der Spoel, D.; Hess B.; Lindahl, E., GROMACS 4.5: a high-throughput and highly parallel open source molecular simulation toolkit. *Bioinformatics,* **2013**, *29*, 845-854, DOI: 10.1093/bioinformatics/btt055.

[26] van Gunsteren, W. F.; Billeter, S. R.; Eising, A. A.; Huenberger, P. H.; Kruger, P.; Mark, A. E.; Scott, W. R. P.; Tironi, I. G., Biomolecular Simulation: the GROMOS 96 Manual and User Guide, Switzerland, 1996.

[27] Darden, T.; York, D.; Pedersen, L., Particle mesh Ewald: An N-log(N) method for Ewald sums in large systems. *J. Chem. Phys.* **1993**, *98*, 10089, DOI: 10.1063/1.464397.

[28] Berendsen, H. J. C.; Postma, J. P. M.; Van Gunstetren, W. F.; Hermans, J., Interaction models for water in relation to protein hydration. In: Pullman B (ed) Intermolecular forces. Reidel, Dordrecht. The Netherlands, 1981, pp. 331-342.

[29] Schuttelkopef, A. W.; wan Aalten, D. M., PRODRG: a tool for high-throughput crystallography of protein-ligand complexes. *Acta Crystallogr. D* **2004**, *60*, 1355-1363, DOI: 10.1107/S0907444904011679.

[30] HyperChem, Release 7.0 for Windows, Hypercube, Inc. 2002.

[31] Karaman, R.; Dajani, K. K.; Qtait, A.; Khamis, M., Prodrugs of acyclovir-a computational approach. *Chem. Biol. Drug Des.* **2012**, *79*, 819-834, DOI: 10.1111/j.1747-0285.2012.01335.x.

[32] Streitwieser, A., Molecular Orbital Theory for Organic Chemists, Wiley, 1961.

[33] Shen, G. F.; Liu, T. T.; Wang, Q.; Jiang, M.; Shi, J. H., Spectroscopic and molecular docking studies of binding interaction of gefitinib, lapatinib and sunitinib with bovine serum albumin (BSA). *J. Photochem. Photobiol. B* **2015**, *153*, 380-390, DOI: 10.1016/j-jphotobiol.2015.10.023.

[34] Zhoua, X.; Yanga, Q.; Xiea, X.; Hua, Q.; Qi, F.; Rahmana, Z. U.; Chen, X., NMR, multi-spectroscopic and molecular modeling approach to investigate the complexes between C.I. Acid Orange 7 and human serum albumin *in vitro*. *Dyes Pigm.* **2012**, *92*, 1100-1107, DOI: 10.1016/j.dyepig.2011.08.012.

[35] Ross, P. D.; Subramanian, S., Thermodynamics of protein association reactions: forces contributing to stability. *Biochemistry* **1981**, *20*, 3096-3102, DOI: 10.1021/BI00514a017.

[36] Lakowicz, J. R., Principles of Fluorescence Spectroscopy, Springer, 2006.

[37] Guozhen, C.; Xianzhi, H.; Jingou, X.; Zunben, W., Methods of Fluorescence Analysis, Science Press, 1990, pp. 112-145.

[38] Wang, T.; Xiang, B.; Wang, Y.; Chen, C.; Dong, Y.; Fang, H.; Wang, M., Spectroscopic investigation on the binding of bioactive pyridazinone derivative to human serum albumin and molecular modeling. *Colloid. Surface. B* **2008**, *65*, 113-119, DOI: 10.1016/j.colsurfb.2008.03.008.

[39] Matei, I.; Ionescu, S.; Hillebrand, M., Interaction of fisetin with human serum albumin by fluorescence, circular dichroism spectroscopy and DFT calculations: binding parameters and conformational changes. *J. Lumin.,* **2011**, *131*, 1629-1635, DOI: 10.1016/j.jlumin.2011.03.073.

[40] Gao, H.; Lei, L.; Liu, J.; Qin, K.; Chen, X.; Hu, Z., The study on the interaction between human serum albumin and a new reagent with antitumour activity by spectrophotometric methods. *J. Photochem. Photobiol. A* **2004**, *167*, 213-221, DOI: 10.1061/ j.jphotochem.2004.05.017

[41] Mandeville, J. S.; Froehlich, E.; Tajmir-Riahi, H. A.; Study of curcumin and genistein interactions with human serum albumin. *J. Pharmaceut. Biomed.* **2009**, *49.2*, 468-474, DOI: 10.1016/J.JPBA.2008.11.035.

[42] Liu, X. F.; Xia, Y. M.; Fang, Y., Effect of metal ions on the interaction between bovine serum albumin and berberine chloride extracted from a traditional Chinese Herb coptis chinensis franch. *J. Inorg. Biochem.* **2005**, *99*, 1449-1457, DOI: 10.1016/ j.jinorgbio.2005,02.025.

[43] Bronowska Agnieszka, K., Thermodynamics of Ligand-protein Interactions: Implications for Molecular Design, Heidelberg Institute for Theoretical Studies Heidelberg, Germany, 2011.

[44] Safarnejad, A.; Shaghaghi, M.; Dehghan, G.; Soltani, S., Binding of carvedilol to serum albumins investigated by multi-spectroscopic and molecular modeling methods. *J. Lumin.* **2016**, *176*, 149-158, DOI: 10.1016/ J.JLUMIN.2 916.02.001.

[45] Yildirim, A., Tekpinar, M., Molecular dynamics investigation of Helicobacter pylori chemotactic protein CheY1 and two mutants. *J. Mol. Model,* **2014**, *20*, 2212, DOI: 10.1007/s00894-014-2212-x.

[46] Curry, S.; Mandelkow, H.; Brick, P.; Franks, N., Crystal structure of human serum albumin complexed with fatty acid reveals an asymmetric distribution of binding sites. *Nat. Struct. Biol.* **1998**, *5*, 827-835, DOI: 10.1038/1869.

[47] Lobanov, M.; Bogatyreva, S.; Galzitskaya, V., Radius of gyration as an indicator of protein structure compactness. *Mol. Biol.* **2008**, *42*, 623-628.

[48] Qais, F.; Abdullah, K. M.; Alam, M. M.; Naseem, I.; Ahmad, I., Interaction of capsaicin with calf thymus DNA: A multi-spectroscopic and molecular modelling study. *Int. J. Biol. Macromol.* **2017**, *97*, 392-402. DOI: 10.1016/j.ijbiomac.2017.01.022.

[49] Morris, G. M.; Goodsell, D. S.; Halliday, R. S.; Huey, R.; Hart, W. E.; Belew, R. K.; Olson, A. J., Automated docking using a Lamarckian genetic algorithm and an empirical binding free energy function. *J. Comput. Chem.* **1998**, *19*, 1639-62. DOI: 10.1002/(SICI)1096-987X(19981115)19

[50] Wallace, A. C.; Laskowski, R. A.; Thornton, J. M., LIGPLOT: a program to generate schematic diagrams of protein-ligand interactions, *Protein Eng.* **1995**, *8*, 127-134, DOI: 10.1093/protein/8.2.